

Simultaneous estimation of arterial and venous oxygen saturation using a camera

Mark van Gastel^a, Hangbing Liang^a, Sander Stuijk^a, and Gerard de Haan^b

^aDepartment of Electrical Engineering, Eindhoven University of Technology, PO Box 513, Eindhoven, The Netherlands

^bPhilips Research, High Tech Campus 34, Eindhoven, The Netherlands

ABSTRACT

Optical monitoring of arterial blood oxygenation, SpO₂, using cameras has recently been shown feasible by measuring the relative amplitudes of the remotely sensed PPG waveforms captured at different wavelengths. SvO₂ measures the venous blood oxygenation which together with SpO₂ provides an indication of tissue oxygen consumption. In contrast to SpO₂ it usually still requires a blood sample from a pulmonary artery catheter. In this work we present a method which suggests simultaneous estimation of SpO₂ and SvO₂ with a camera. Contrary to earlier work, our method does not require external cuffs leading to better usability and improved comfort. Since the arterial blood varies synchronously with the heart rate, all frequencies outside the heart rate band are typically filtered out for SpO₂ measurements. For SvO₂ estimation, we include intensity variations in the respiratory frequency range since respiration modulates venous blood due to intrathoracic pressure variations in the chest and abdomen. Consequently, under static conditions, the two dominant components in the PPG signals are respiration and pulse. By measuring the amplitude ratios of these components, it seems possible to monitor both SpO₂ and SvO₂ continuously. We asked healthy subjects to follow an auditory breathing pattern while recording the face and hand. Results show a difference in estimated SpO₂ and SvO₂ values in the range 5-30 percent for both anatomical locations, which is normal for healthy people. This continuous, non-contact, method shows promise to alert the clinician to a change in patient condition sooner than SpO₂ alone.

Keywords: Remote sensing, infrared, blood oxygen saturation, SpO₂, SvO₂

1. INTRODUCTION

After reported successes showing camera-based pulse rate and derived features such as HRV, respiration and PPG imaging (PPGI), the optical measurement of arterial blood oxygenation, SpO₂, is rapidly gaining interest from the research community and industry¹ because of its clinical importance for the evaluation of proper respiratory function. SpO₂ can be determined from multi-wavelength PPG signals based on the absorption differences between oxyhemoglobin (HbO₂) and (reduced) hemoglobin (Hb). Since the absorption spectrum of the blood indicates the oxygenation level, while only the arterial blood pulsates at the pulse rate frequency, the arterial oxygenation level can be estimated by comparing the relative pulsatile amplitudes at different wavelengths. After some initial attempts,²⁻⁵ the feasibility of calibrateable camera-based SpO₂ has first been demonstrated by Verkruysse *et al.*⁶ using hypoxic conditions. Compared to conventional contact-mode PPG, the amplitude of the remotely sensed PPG signal is much smaller and consequently more vulnerable to noise and motion artifacts. Because of this Van Gastel *et al.*⁷ proposed an indirect method which enables robust SpO₂ estimation on noisy and motion-corrupted PPG waveforms.

In contrast to SpO₂, monitoring of mixed venous blood oxygenation, SvO₂, usually still requires a blood sample from a pulmonary artery catheter with its associated risks. This is because peripheral venous saturations cannot replace or infer SvO₂ and the cardiac-periodic blood volume variations used to isolate the absorbance of arterial blood from other absorbers is absent for venous blood. It is therefore unclear which portion of the reflected light originates from venous blood. The assessment of SvO₂ in the skin or muscle can provide information on the adequacy of local blood flow,⁸ whereas SpO₂ only gives information about the incoming supply

Send correspondence to M. van Gastel
E-mail: m.j.h.v.gastel@tue.nl

of oxygen. Low values of skin blood flow can indicate the occurrence of shock or cardiac failure, in which blood flow is diverted from the peripheral circulation toward more vital organs. Venous blood concentrations can be changed by applying external pressure and occluding the draining veins, by changing tissue level relative to the heart. Venous walls are significantly thinner and less elastic than arterial walls. In particular, the veins are up to 10-20 times more compliant compared to arteries under low pressure.⁹ With relatively small changes in pressure, the circulating blood inside the much more compliant veins experiences large volume changes compared to the arteries.¹⁰ Hence, this compliance difference can be exploited to artificially induce modulations at respiratory frequency and low pressure in the venous system, without disturbing arterial blood flow,¹¹ which can be measured using PPG. Zhang *et al.*¹² and Khan *et al.*¹³ proposed a non-invasive SvO₂ measurement method where a cyclic pressure stimulus is applied to the finger by means of a strain gauge. Using the common ratio-of-ratios approach, they reported optical SvO₂ measurements in the range 71 – 86%, whereas the gold-standard SvO₂ values based on venous blood gas measurements were in a similar range, 74 – 88%.

Instead of applying a cyclic pressure stimulus and estimate the venous oxygenation based on the stimuli-synchronous intensity variations, another proposed measurement methodology is to apply a static pressure to a limb to prevent venous outflow, often referred to as venous occlusion. Apart from contact-based approaches based on this principle,¹⁴ a camera-based SvO₂ imaging approach has been proposed by Li *et al.*¹⁵ Their method requires an external cuff attached to the upperarm which applies a pressure to prevent venous return from the arm back to the heart. The venous oxygenation level is determined based on the baseline intensity variation during venous occlusion resulting in SvO₂ estimates consistent with those reported in literature. Although by applying an external pressure it is possible to isolate the absorption of the venous blood from other absorbers, it does not allow continuous measurement and the required disturbance to the local physiology could lead to complications such as venous stasis and thrombosis. It is therefore not used in daily practise. Furthermore, the amount of pressure required, high enough to modulate or block venous blood and low enough to not affect arterial blood, is not easily determined.

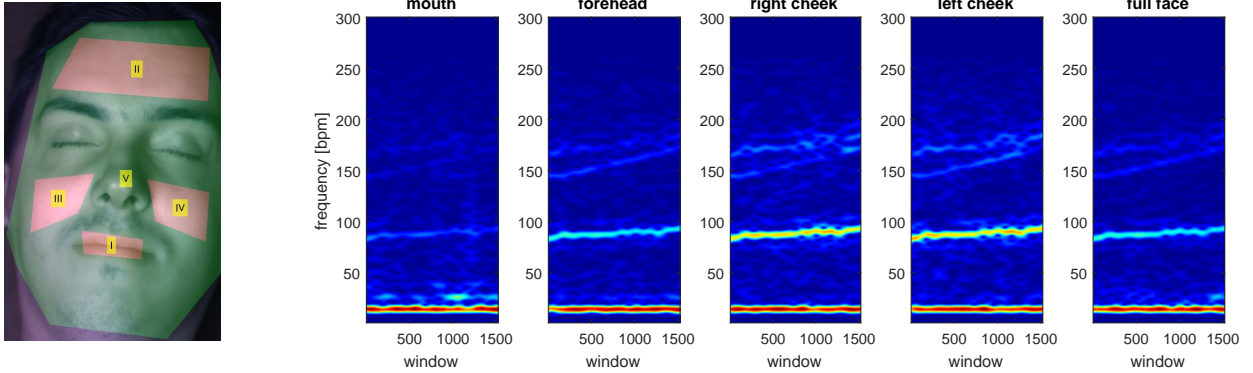
Internal pressure sources are the lungs inducing the respiratory-synchronous baseline modulation of the PPG signal. By extracting this modulation from the PPG waveform respiratory rate and volume data can be derived as has been shown with a finger-oximeter¹⁶ and with a camera.¹⁷ Based on the assumption that the change in tissue blood volume which gives rise to respiratory-induced changes in the PPG waveform arises from transmitted reduction in venous pressure due to negative intrathoracic pressures, Franceschini *et al.* developed a measurement methodology denoted as “spiroximetry”.¹⁸ Based on measurements on the oscillatory component at the respiratory frequency, good agreement was found between optical SvO₂ estimates and SvO₂ on blood samples on pigs with an average difference of 1%. They also studied the difference between SvO₂ estimates based on respiration and venous occlusion and found an average deviation of 0.8% with maximum discrepancies of -4.2 and 5.8%, which indicates that respiration can serve as a replacement for the external cuff to modulate venous blood. Based on the same principle, venous saturation estimates have later been obtained from oesophageal¹⁹ and peripheral²⁰ PPG signals. In the remainder of this paper we will use the notation SxvO₂ for the optical estimation of SvO₂ to avoid confusion and possible wrong interpretation of the results.

In the present exploratory study we investigate the feasibility of using a camera for continuous and simultaneous estimation of arterial and local venous oxygen saturation without applying an external pressure stimulus. Instead we use respiration as an internal pressure source to modulate venous blood periodically from which venous oxygenation levels can be derived from multiple skin-sites simultaneously. A simultaneous estimation of arterial and venous oxygen saturation potentially allows continuous estimation of local oxygen consumption and early detection of septic shock. In Section 2, we provide details of the study design, experimental setup and data processing. Section 3 presents the results, which are discussed in Section 4. Finally, our conclusions are presented in Section 5.

2. MATERIALS AND METHODS

2.1 Study Design

In this exploratory study we enrolled three healthy subjects, 2 males and 1 female, with an age in the range 26-31 years. The subjects are recorded in supine position and are asked to follow an auditory breathing pattern with a fixed frequency of 12 breaths/min for the duration of 3 minutes for easy identification of the respiratory



(a) Facial ROIs created from landmarks

(b) Spectrograms facial ROIs

Figure 1: Using the facial landmarks, five ROIs are created from locations with high pulsatile amplitudes (a), from which pulse-signals are extracted (b).

frequencies. Institutional Review Board approval and informed consent were obtained prior to measurements. A multi-spectral camera, type Fluxdata FD-1665-MS3 with 15 fps sampling frequency, 782x582 pixels resolution and a 50mm lens was used for the data collection. The center wavelengths of the three channels are 760, 800 and 890nm, with 25nm, 25nm and 50nm bandwidth, respectively. A lamp holder with 9 identical incandescent light bulbs is placed above the subject’s face at a distance of 1.5 meter to provide diffuse homogeneous illumination. Incandescent light is chosen because it provides a continuous spectrum and covers all wavelengths of the camera. A reference finger-probe is connected to a Philips IntelliVue MP50 which logs the red and infrared plethysmograms together with the derived pulse rates and oxygenation levels. The camera and IntelliVue MP50 are connected to an acquisition notebook where the camera and reference data is stored synchronously and uncompressed.

2.2 Image and Signal Processing

From the video frames we would like to estimate SpO_2 and $SxvO_2$ values from different anatomical locations with high pulsatile amplitudes on both the face and hand;^{21, 22} mouth, forehead, cheeks, full face and palm. For the face, facial landmarks are detected from the full-frame image which are subsequently used to generate ROIs using polygonization. The pixels within the ROIs are averaged for the three color channels to overcome sensor and quantization noise. The procedure is visualized in Fig. 1. For the hand, the palm is manually selected at initialization.

A cardiac pulse signal can be expressed as a linear combination of DC-normalized color channels contaminated with noise:

$$\tilde{\mathbf{S}} = \vec{W} \mathbf{C}_n + \eta, \quad (1)$$

where \vec{W} denotes the weights and \mathbf{C}_n is a matrix containing the DC-normalized color signals. To find the weights for \vec{W} , various methods have been proposed, which can roughly be classified into 1) BSS-based methods using heuristics to select the pulse signal from the other signals,^{23, 24} 2) methods which exploit the known characteristics of the typical distortions,^{25, 26} and 3) methods using prior knowledge about the relative pulse amplitudes.²⁷ Since the prior of the later approach is SpO_2 -dependent the method can be extended to enable robust SpO_2 measurements, denoted as APBV:⁷

$$SpO_2 = \underset{SpO_2 \in \mathbf{SpO}_2}{\operatorname{argmax}} \operatorname{SNR} \left(\overbrace{k \vec{P}_{bv}(SpO_2) [\mathbf{C}_n \mathbf{C}_n^T]^{-1} \mathbf{C}_n}^{\vec{W}_{PBV}} \right), \quad (2)$$

where $\vec{P}_{bv}(SpO_2)$ denotes the pulse vector and k is a scalar to scale the weights to unit length. Instead of extracting features from the individual PPG waveforms, a single pulse signal is created as a linear combination

of the PPG waveforms using the SpO₂-dependent pulse ‘signature’ prior. The benefit of this approach is the ability to suppress distortions enabling robust pulse rate detection whilst the optimum corresponding to the SpO₂ value remains stable. Essentially, by searching for the pulse vector that provides the best pulse signal in terms of SNR, the oxygenation level can be determined. A consequence of the SNR-based selection criterion is that cardiac-similar frequencies, e.g. ballistocardiography (BCG), influence the measurement. Similarly, we expect respiratory motions to affect our estimate of the SxvO₂ measurement. Under uniform, homogeneous illumination we know that these motions cause intensity variations equal in all color channels, which can be expressed by the mixing vector $\mathbf{1}$. We therefore propose to apply a projection on a plane orthogonal to this distortion on the DC-normalized signals to eliminate motion artifacts before oxygenation levels are estimated. This projection should therefore satisfy:

$$\mathbf{P} \cdot \vec{\mathbf{1}} = 0. \quad (3)$$

This projection should consequently also be applied to the SpO₂ calibration model, $\vec{P}_{bv}(SpO_2)$, used for pulse extraction:

$$SpO_2 = \underset{SpO_2 \in \mathbf{SpO}_2}{\operatorname{argmax}} \operatorname{SNR} \left(\overbrace{k\mathbf{P}\vec{P}_{bv}(SpO_2)[\mathbf{C}\mathbf{P}_n\mathbf{C}\mathbf{P}_n^T]^{-1}\mathbf{C}\mathbf{P}_n}^{\vec{W}_{PBV}} \right), \quad (4)$$

where $\mathbf{C}\mathbf{p}_n = \mathbf{P}\mathbf{C}_n$. A consequence of the projection is that the pulse amplitudes are lower compared to the amplitudes before projection and noise is boosted. Dependent on the projection the two projected signals could also be in anti-phase for certain oxygenation levels. This is problematic for the conventional ratio-of-ratios method but it has a much less detrimental effect on the performance of APBV. Since we have the freedom to use any projection on the plane orthogonal to $\mathbf{1}$, we determined our projection based on two criteria; 1) pulse amplitude and 2) SpO₂ contrast, indicated with F^p and F^c , respectively:

$$\begin{aligned} F^p(\Theta) &= \overline{\left(\sum_{SpO_2 \in \mathbf{SpO}_2} |R(\theta)\mathbf{P}\vec{P}_{bv}(SpO_2)| \right)} \\ F^c(\Theta) &= \left(\frac{\partial P_{bv}^{p,1}}{\partial S P_{bv}^{p,2}} \right), \text{ with } \begin{bmatrix} P_{bv}^{p,1} \\ P_{bv}^{p,2} \end{bmatrix} = R(\theta)\vec{P}_{bv}(SpO_2) \quad \forall SpO_2 \in \mathbf{SpO}_2, \end{aligned} \quad (5)$$

where $\overline{}$ is the sample mean operator and $\frac{\partial}{\partial S}$ the derivative with respect to oxygenation levels. Since APBV can only cope with linear relations such as pulse and motion, and not with uncorrelated noise, e.g. sensor noise, we would like to have signals with reasonable pulse amplitude after projection. Furthermore, we would like to have a reasonable SpO₂ *contrast*, which we specify as the change in absorption as function of oxygenation levels. A large contrast allows to detect small changes in oxygen saturation. In order to find the optimal projection, we rotate an initial projection on the plane orthogonal to $\mathbf{1}$ and evaluate the values of our criteria, as visualized in Fig. 2.

When giving equal weights to both optimization criteria and evaluating oxygenation levels in the expected range [60 – 100]%, the optimal projection is found to be $\mathbf{P} = \begin{bmatrix} -1.0465 & 0.9459 & 0.1006 \\ -0.8452 & -1.1472 & 1.9924 \end{bmatrix}$. An illustration of this projection applied on data obtained on the forehead is visualized in Fig. 3. The projection is applied to two differently band-pass filtered versions of the DC-normalized signals; 1) filtered for respiration, and 2) filtered for pulse. Respiratory frequencies lower than 10 breaths/min. are eliminated since these interfere with Traube-Hering-Mayer (THM) waves, whereas higher frequencies interfere with pulse. An overview of the processing framework is visualized in Fig. 4. Estimates of arterial and venous saturation levels are finally obtained using our earlier introduced and modified APBV method, Eq. 4. We used time-windows of 20 seconds, a step-size of 1 second and a 10th-order Butterworth filter for band-pass filtering. Each time-window was used to calculate arterial and venous oxygen saturation estimates.

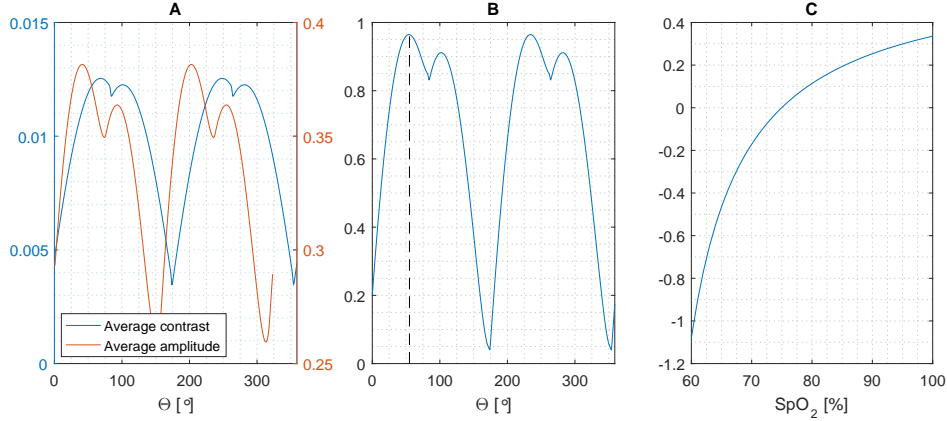


Figure 2: A) values of two optimization criteria for rotations on the plane orthogonal to intensity variations, B) value of the combined, equally weighted optimization features where the dashed line indicates the optimum, C) the calibration curve for the optimal projection.

3. RESULTS

The arterial blood oxygenation and the local venous blood oxygenation results are displayed in Fig. 5a and Fig. 5b, respectively. The finger-oximeter allows performance evaluation for SpO_2 , whereas due to the unavailability of the gold-standard blood gas analysis, the estimated SvO_2 values can only be compared to values reported in literature and checked for consistency for the different ROIs. As can be observed from Fig. 5a, the medians of all locations are in large agreement for the SpO_2 estimates and in agreement with the contact-based reference. Evaluation metrics calculated by comparing the remote estimates with the finger-oximeter are displayed in Table 1. Although differences are small, the mouth and cheek areas have a larger error when compared to the other evaluated skin locations, which is likely caused by the smaller number of pixels within the ROI affecting the pulse quality. The SvO_2 estimates are fairly equal for the facial ROIs, although they show larger deviations compared to the SpO_2 estimates. The estimated venous saturation on the palm is higher compared to the facial regions, which is especially noticeable for subject III. The camera-based measurements are within the physiological range

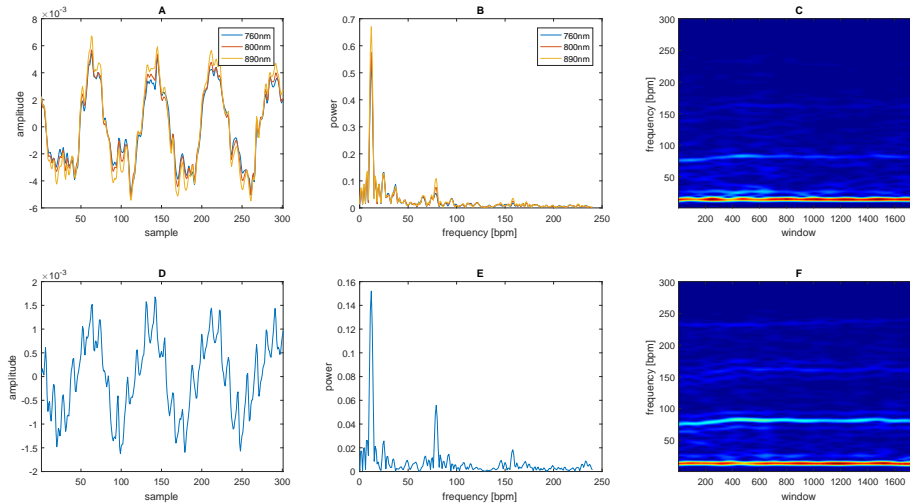


Figure 3: A) DC-normalized signals from the 3 channels, B) corresponding spectra with peaks at both breathing and pulse rate, C) spectrogram 890nm channel from the full recording, D) signal after projection to eliminate motion artifacts, E) corresponding spectrum after amplitude tuning, F) spectrogram from the full recording.

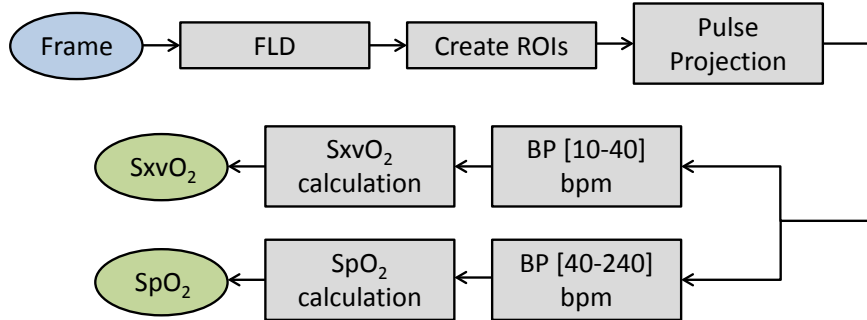


Figure 4: Processing pipeline for simultaneous SxvO₂ and SpO₂ estimation. For each frame Facial Landmark Detection (FLD) is performed from which temporally-consistent ROIs covering different parts of the face can be created. Pulse signals are extracted from each ROI and after DC-normalization projected on a plane orthogonal to **1** to eliminate motion artifacts which potentially corrupt the measurement. Hereafter the 2 projected signals are band-pass (BP) filtered with two different filters; 1) a BP which includes respiratory frequencies, 2) a BP filter which includes pulse frequencies. Finally the SxvO₂ and SpO₂ values are obtained with the indirect APBV method.⁷

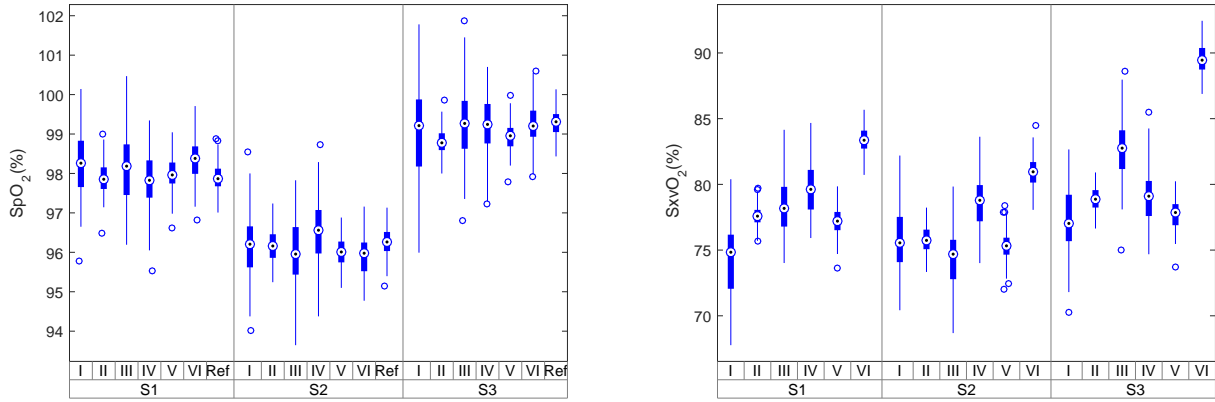
of venous saturations and consistent with those reported in literature.

Table 1: Results SpO₂ estimates from different skin sites when compared with the reference finger pulse-oximeter. Evaluation metrics are the Mean Absolute Error (MAE), Bias (B) and standard deviation (σ)

ROI	S1			S2			S3		
	MAE	B	σ	MAE	B	σ	MAE	B	σ
I - Mouth	0.776	0.361	0.878	0.760	-0.0817	0.946	0.956	-0.225	1.13
II - Forehead	0.473	-0.0185	0.601	0.419	-0.0804	0.515	0.570	-0.507	0.451
III - Right cheek	0.848	0.264	0.993	0.758	-0.295	0.934	0.784	-0.0209	0.978
IV - Left cheek	0.647	-0.058	0.805	0.722	0.273	0.879	0.659	-0.102	0.818
V - Full face	0.439	0.0960	0.551	0.463	-0.251	0.543	0.478	-0.348	0.490
VI - Hand	0.632	0.435	0.656	0.609	-0.335	0.645	0.500	-0.0408	0.619

4. DISCUSSION

The measurement principle assumes the respiratory modulations present in the PPG signals to originate from venous blood only. Earlier studies showed this assumption to hold when comparing the optical SvO₂ estimates with measurement obtained on venous blood samples.¹⁸ However, it has also been reported that macrocirculation is not the sole determinant of respiratory induced variations in the reflection mode photoplethysmographic signal.²⁸ Nilsson *et al.* studied the coherence between the respiratory induced intensity variations (RIIVs) of the PPG signal and respiratory synchronous pressure variations in central venous pressure (CVP), peripheral venous pressure (PVP) and arterial blood pressure (ABP) during positive pressure ventilation on 12 patients under anaesthesia and on 12 patients with spontaneous breathing. The phase relation between RIIV and respiratory induced variation in macrocirculation changed with ventilatory mode, but not in a uniform way, indicating the influence of mechanisms other than macrocirculation involved in generating the RIIV signal and therefore influencing the outcome of the SxvO₂ measurement. It has been argued that sympathetically mediated vasoconstriction from respiratory-synchronous discharge of the autonomic nervous system also plays a role, which can affect the PPG waveform independently of the changes resulting from the mechanical effects of the respiratory cycle. Nitzan *et al.*²⁹ studied the PPG waveform obtained from a finger probe placed distal to an artery occluded by a blood pressure cuff inflated above systolic pressure to exclude the possibility that the change in waveform



(a) Arterial oxygen saturation

(b) Venous oxygen saturation

Figure 5: Estimated SpO_2 and SvO_2 values measured at the six ROIs (I=mouth, II=forehead, III=right cheek, IV=left cheek, V=full face, VI=palm) for the three subjects (S).

was transmitted intravascularly from mechanical changes in the thoracic cavity. A variation in the baseline of the PPG waveform was evident during a deep inspiratory gasp but not during normal respiration, suggesting a coupling of the respiratory system to the autonomic nervous system.

In our study we asked healthy subjects to follow an auditory breathing pattern. In their study, Belhaj *et al.*³⁰ observed a large difference in estimated SvO_2 values between spontaneously-breathing volunteers and mechanically ventilated anaesthetised patients when compared with co-oximetry samples of venous blood from the dorsum of the hand. This suggests that cutaneous arteriovenous shunt induced by anaesthesia may especially limit the use of this technique in anaesthetised patients. It has also been reported that during mechanical ventilation the amplitude of the RIIVs are inversely proportional to CVP.³¹ Besides the differences between natural breathing and ventilation, the presence and degree of respiratory-synchronous baseline modulation in the PPG signals extracted from the upper part of the body will also be affected by the type of breathing and air volume.²⁸

Although a completely non-contact measurement principle is advantageous in terms of patient comfort compared to methods which require external stimuli, a disadvantage of PPG-based approaches is the requirement of the detectability of the cardiac-similar and respiratory-similar modulations. This somehow limits the application to skin sites with high arteriolar/venular density and consequently a relatively strong pulse/respiratory signal, e.g. the face and palm. The venous occlusion methods enable generation of high-resolution SxvO_2 maps as has been demonstrated by Li *et al.*¹⁵ Because the cuff was applied for up to 30 seconds on both the wrist and just above the elbow, larger variations in venous blood volume can be realized compared to periodic stimuli, resulting in larger intensity variations. This approach may therefore be favourable for SxvO_2 imaging applications, especially for skin sites with relatively low arteriolar/venular density.

This exploratory study showed that our measurements lead to oxygenation estimates that are in the expected range of SvO_2 . This warrants follow up studies using a reference measurement of SvO_2 to check that these values are actually meaningful. It is especially important to verify if the temporal and spatial variations in estimated SxvO_2 are consistent with the reference or that these are attributable to other factors, contradicting our current assumption that RIIVs originate solely from variations in venous blood. A successful validation warrants an investigation on the feasibility of SxvO_2 estimation during spontaneous instead of guided breathing, which introduces the additional challenge identifying which frequency components are related to breathing required for the SNR calculation of the APBV method. By combining the local venous saturation estimates from multiple skin-sites, it may be possible to generate a surrogate for the true mixed venous saturation.

5. CONCLUSION

In this study regional venous oxygenation was estimated by utilising the respiratory modulations present in the PPG signals without the need to apply external pressure stimuli. This was combined with our earlier proposed SpO₂ method enabling simultaneous and continuous estimation of arterial and venous blood oxygenation. To eliminate motion artifacts with cardiac-similar and/or respiration-similar frequency we proposed to eliminate these prior to the oxygen saturation estimation. The results of the exploratory study on healthy subjects show similar and spatially-consistent SpO₂ estimates for the evaluated skin sites, whereas the estimated SxvO₂ values are consistent with those reported in literature. The results are encouraging and show the promise of the non-contact measurement principle, although validation on a larger population and with the invasive gold-standard is required to quantify the accuracy of the SxvO₂ estimation.

ACKNOWLEDGMENTS

The authors are grateful for the help and contributions of their Philips colleagues B. Balmaekers, P. Bruins and all volunteers who participated in the experiments.

REFERENCES

- [1] <https://www.philips.com/a-w/about/news/archive/standard/news/press/2016/20160606-philips-proprietary-camera-based-monitoring-technology-is-first-in-the-world-to-measure-absolute-arterial-blood-oxygenation-levels-without-ever-touching-the-patient.html>.
- [2] Wieringa, F. P., Mastik, F., and van der Steen, A. F., “Contactless multiple wavelength photoplethysmographic imaging: a first step toward spo₂ camera technology,” *Annals of Biomedical Engineering* **33**(8), 1034–1041 (2005).
- [3] Humphreys, K., Ward, T., and Markham, C., “Noncontact simultaneous dual wavelength photoplethysmography: a further step toward noncontact pulse oximetry,” *Review of Scientific Instruments* **78**(4), 044304 (2007).
- [4] Kong, L., Zhao, Y., Dong, L., Jian, Y., Jin, X., Li, B., Feng, Y., Liu, M., Liu, X., and Wu, H., “Non-contact detection of oxygen saturation based on visible light imaging device using ambient light,” *Optics Express* **21**(15), 17464–17471 (2013).
- [5] Tarassenko, L., Villarroel, M., Guazzi, A., Jorge, J., Clifton, D., and Pugh, C., “Non-contact video-based vital sign monitoring using ambient light and auto-regressive models,” *Physiological Measurement* **35**(5), 807 (2014).
- [6] Verkruyse, W., Bartula, M., Bresch, E., Rocque, M., Meftah, M., and Kirenko, I., “Calibration of contactless pulse oximetry,” *Anesthesia & Analgesia* **124**(1), 136 (2017).
- [7] Van Gastel, M., Stuijk, S., and De Haan, G., “New principle for measuring arterial blood oxygenation, enabling motion-robust remote monitoring,” *Scientific Reports* **6**, 38609 (2016).
- [8] Nitzan, M. and Taitelbaum, H., “The measurement of oxygen saturation in arterial and venous blood,” *IEEE Instrumentation & Measurement Magazine* **11**(3) (2008).
- [9] Caro, C. G., [*The mechanics of the circulation*], Cambridge University Press (2012).
- [10] Wardhan, R. and Shelley, K., “Peripheral venous pressure waveform,” *Current Opinion in Anesthesiology* **22**(6), 814–821 (2009).
- [11] Groothuis, J. T., van Vliet, L., Kooijman, M., and Hopman, M. T., “Venous cuff pressures from 30 mmhg to diastolic pressure are recommended to measure arterial inflow by plethysmography,” *Journal of Applied Physiology* **95**(1), 342–347 (2003).
- [12] Zhang, X., Zhang, M., Zheng, S., Wang, L., and Ye, J., “A new method for noninvasive venous blood oxygen detection,” *Biomedical Engineering Online* **15**(1), 84 (2016).
- [13] Khan, M., Pretty, C. G., Amies, A. C., Balmer, J., Banna, H. E., Shaw, G. M., and Chase, J. G., “Proof of concept non-invasive estimation of peripheral venous oxygen saturation,” *Biomedical Engineering Online* **16**(1), 60 (2017).

- [14] Yoxall, C. and Weindling, A., “Measurement of venous oxyhaemoglobin saturation in the adult human forearm by near infrared spectroscopy with venous occlusion,” *Medical and Biological Engineering and Computing* **35**(4), 331–336 (1997).
- [15] Li, J., Dunmire, B., Beach, K. W., and Leotta, D. F., “A reflectance model for non-contact mapping of venous oxygen saturation using a ccd camera,” *Optics Communications* **308**, 78–84 (2013).
- [16] Johansson, A. and Öberg, P., “Estimation of respiratory volumes from the photoplethysmographic signal. part i: experimental results,” *Medical and Biological Engineering and Computing* **37**(1), 42–47 (1999).
- [17] van Gastel, M., Stuijk, S., and de Haan, G., “Robust respiration detection from remote photoplethysmography,” *Biomedical Optics Express* **7**(12), 4941–4957 (2016).
- [18] Franceschini, M. A., Boas, D. A., Zourabian, A., Diamond, S. G., Nadgir, S., Lin, D. W., Moore, J. B., and Fantini, S., “Near-infrared spirometry: noninvasive measurements of venous saturation in piglets and human subjects,” *Journal of Applied Physiology* **92**(1), 372–384 (2002).
- [19] Walton, Z. D., Kyriacou, P. A., Silverman, D. G., and Shelley, K. H., “Measuring venous oxygenation using the photoplethysmograph waveform,” *Journal of Clinical Monitoring and Computing* **24**(4), 295–303 (2010).
- [20] Thiele, R. H., Tucker-Schwartz, J. M., Lu, Y., Gillies, G. T., and Durieux, M. E., “Transcutaneous regional venous oximetry: a feasibility study,” *Anesthesia & Analgesia* **112**(6), 1353–1357 (2011).
- [21] Verkruyse, W., Svaasand, L. O., and Nelson, J. S., “Remote plethysmographic imaging using ambient light,” *Optics Express* **16**(26), 21434–21445 (2008).
- [22] Lempe, G., Zaunseder, S., Wirthgen, T., Zipser, S., and Malberg, H., “ROI selection for remote photoplethysmography,” in [*Bildverarbeitung für die Medizin 2013*], 99–103 (2013).
- [23] Poh, M.-Z., McDuff, D. J., and Picard, R. W., “Advancements in noncontact, multiparameter physiological measurements using a webcam,” *Biomedical Engineering, IEEE Transactions on* **58**(1), 7–11 (2011).
- [24] Lewandowska, M., Ruminski, J., Kocejko, T., and Nowak, J., “Measuring pulse rate with a webcam - a non-contact method for evaluating cardiac activity,” in [*Computer Science and Information Systems (FedCSIS), 2011 Federated Conference on*], 405–410 (2011).
- [25] de Haan, G. and Jeanne, V., “Robust pulse-rate from chrominance-based rPPG,” *Biomedical Engineering, IEEE Transactions on* **60**(10), 2878–2886 (2013).
- [26] Wang, W., den Brinker, A. C., Stuijk, S., and de Haan, G., “Algorithmic principles of remote ppg,” *IEEE Transactions on Biomedical Engineering* **64**(7), 1479–1491 (2017).
- [27] de Haan, G. and van Leest, A., “Improved motion robustness of remote-PPG by using the blood volume pulse signature,” *Physiological Measurement* **3**(9), 1913–1926 (2014).
- [28] Nilsson, L., Johansson, A., and Kalman, S., “Macrocirculation is not the sole determinant of respiratory induced variations in the reflection mode photoplethysmographic signal,” *Physiological Measurement* **24**(4), 925 (2003).
- [29] Nitzan, M., Faib, I., and Friedman, H., “Respiration-induced changes in tissue blood volume distal to occluded artery, measured by photoplethysmography,” *Journal of Biomedical Optics* **11**(4), 040506–040506 (2006).
- [30] Belhaj, A., Phillips, J., Kyriacou, P., and Langford, R., “Comparison of non-invasive peripheral venous saturations with venous blood co-oximetry,” *Journal of clinical monitoring and computing* **31**(6), 1213–1220 (2017).
- [31] Dorlas, J. and Nijboer, J., “Photo-electric plethysmography as a monitoring device in anaesthesia: application and interpretation,” *BJA: British Journal of Anaesthesia* **57**(5), 524–530 (1985).